On Antenna Design Objectives and the Channel Capacity of MIMO Handsets

Nielsen, Jesper Ødum; Yanakiev, Boyan; Barrio, Samantha Caporal Del; Pedersen, Gert Frølund

Published in:
I E E E Transactions on Antennas and Propagation

DOI (link to publication from Publisher):
10.1109/TAP.2014.2309967

Publication date:
2014

Document Version
Accepted author manuscript, peer reviewed version

On Antenna Design Objectives and the Channel Capacity of MIMO Handsets

Jesper Ødum Nielsen, Boyan Yanakiev, Samantha Caporal Del Barrio, Gert Frølund Pedersen

***Abstract*—The branch correlation coefficient (BCC), the branch power ratio (BPR), and the total mean power (TMP) are often used to characterize the mobile multiple-input multiple-output (MIMO) channel. This work investigates to which degree these parameters are useful for maximizing the channel capacity of MIMO handheld devices used in data mode. A statistical point of view is applied, using about 2,800 outdoor to indoor channel sounder measurements obtained with combinations of 10 different handsets, 4-8 test users and a variety of different use cases (UCs). All measurements were made in an urban environment in a setup with two different base stations (BSs) and with the users inside a single building. For each measurement combination, the mean capacity (MC) and associated values of BCC, BPR, and TMP are obtained. From the data it is found that the MC is only weakly correlated with both the BCC and the BPR, while the MC is highly correlated with the TMP.**

***Index Terms*—MIMO channels, propagation measurements, channel capacity, branch power ratio, branch correlation, mean effective gain, user-interaction, dual-band propagation, optical link**

I. Introduction

The MIMO transmission technology is well known for its potential to allow for increased transmission capacity compared to that of traditional single-input single-output (SISO) systems [1]. MIMO technology has long been used in *e.g.*, 802.11n wireless local area networks (WLANs) [2] and, more recently, MIMO is an important part of the evolving long-term evolution (LTE) systems [3].

Where WLAN devices in the early days were less likely to be in close contact to the device user, *e.g.*, in laptop usage, typical use of handsets or smartphones, commonly referred to as *handsets* in the following, with both LTE and WLAN, often involve close contact to the user's hand or other parts of the body.

It is well known that the user presence may have a significant influence on the handset performance and depends, *e.g.*, on the type of grip, hand location relative to the body, and orientation with respect to the environment. For example in [4] it is reported that the user presence as modeled by a phantom caused a modest increase in correlation between the antennas, as well as a loss of power of up to 10 dB. The power loss is comparable to what has been reported for SISO terminals, *e.g.*, in [5], [6]. Similarly in [7], using a mockup handset and indoor channel measurements, it was concluded that the presence of a user results in a loss of power but otherwise only has a small influence on diversity and capacity.

The work in [8] is based on simulations of the channel in combinations with either simulated or measured radiation patterns including a phantom hand. Here it was found that the capacity of the channel may be reduced by up to 40% when a user hand is present next to the handset, compared to the free space (FS) case. Also based on simulations of the channel in combination with simulated radiation patterns with and without a simple cylinder model of the user's body, the work in [9] considers the case where the handset is carried in a pocket on the user's body. Here a 10–54% capacity degradation was found compared to the FS case.

The work in [10] and [11] consider the influence of a user on diversity in a handset, based on simulations and measurements of user phantoms. It was found that the correlation is lowered due to the user for frequencies around 870 MHz, but at the same time the power received by the antennas is reduced.

The influence of the channel's cross-polarization ratio (XPR) on the capacity was investigated in [12] for a handset mockup in FS and in front of a user. Using models of the channel, the capacity was found to depend on the channel XPR, as were the mean effective gain (MEG) and branch correlation coefficient (BCC). Furthermore, the user influence lowered the capacity about 40% for all of the frequency bands 800 MHz, 1.7 GHz and 2.0 GHz. Other studies of capacity for mobile terminals include [13]–[16], all based on measurements of the channel, some without user influence.

Although many works are based at least partly on simulations and models, measurement based investigations are essential since the effects of the user and the mobile channel are difficult to include in simulations [15]. The work in [17] is based on numerous propagation channel measurements with mock-up handsets and different users situated in an indoor environment. FS capacities and the influence of users are reported for six different handsets.

In the design of handsets, optimization for high capacity is desirable to get the most from the available frequency spectrum. The capacity of the MIMO channel may be computed for a given signal to noise ratio (SNR) if the eigenvalues of the channel matrix are known [1]. The channel matrix is given by the random propagation channel in combination with the antenna system properties at both ends of the channel, and thus typically is random and must be analyzed in statistical terms. Since the properties of the propagation channel often cannot

J. Ø. Nielsen, B. Yanakiev, S. Caporal Del Barrio, and G. F. Pedersen are with the Antennas, Propagation and Radio Networking section at the Department of Electronic Systems, Faculty of Engineering and Science, Aalborg University, Denmark. B. Yanakiev is also with Intel Mobile Communications, Alfred Nobels Vej 25, DK-9220 Aalborg, Denmark

J. Ø. Nielsen and B. Yanakiev were supported by the Danish National Advanced Technology Foundation via the Converged Advanced Mobile Media Platforms (CAMMP) project. The results and conclusions presented by the authors in this article are not necessarily supported by the other partners of the CAMMP project.

Published in *IEEE Transactions on Antennas and Propagation*, Vol. 62, No. 6, p. 3232–3241, June 2014. DOI: 10.1109/TAP.2014.2309967.

be changed, optimizing for high capacity can be interpreted as a matching of the antenna systems properties to those of the channel. The antennas at the mobile station (MS) end of the link is the focus of the current work.

A key question is how to perform the optimization of the antenna system in a design phase to achieve the maximum capacity in typical channels. In practice high efficiency of the antennas, low correlation and branch power ratio (BPR) (in dB) between antenna branches are commonly aimed for when designing handsets.

It is known that a low BCC is important to obtain diversity and necessary (but not sufficient) to reach the highest capacity [18], [19]. Furthermore, a low BPR and high antenna MEGs are recognized as important for large capacity [20]–[22]. Assuming a known angular power distribution (APD) in the environment, the BCC, BPR, and MEG can all be computed from the radiation patterns of the antennas [23], [24]. Thus, all the parameters can be considered as attempts to reduce the complexity of the radiation patterns of the antenna system into simpler figure of merits. It is then important to study the relevance of each parameter for optimizing the capacity. This was done to some extent in [25], where the correlation predicted at the design stage using environment models was compared to actually measured correlation in both FS and with users. It was concluded that the FS results are significantly different from the with user case; furthermore, optimization of the correlation showed little benefit for the actually achieved capacity.

When considering optimization for high capacity, it should be remembered that capacity is a theoretical measure that can only be achieved in the limit with sufficiently powerful coding and (quasi) static channel conditions that cannot be assumed in actual cellular systems. Taking into account the aspects of realistic cellular systems is possible but requires some assumptions on issues such as user mobility, traffic scheduling, cell loading, and network implementation. The works in [26] and [27] are examples of LTE system simulations including different mockup handsets, in FS and with a phantom for obtaining the throughput. Measurements have also been performed in a deployed, but "pre-commercial", LTE system, as reported in [28] where the throughput has been studied for three handsets in FS and hand phantoms. Other LTE field measurements are reported in [29] where different BS antennas are studied.

Given the important differences, it is interesting to note that the work in [26] reports consistent ranking of four mockup devices using either throughput or capacity measures.

The main contribution of the current work is to analyze from a statistical point of view the link between the capacity and the BCC, BPR, and mean power gain, and thereby determine which parameters are in general most relevant for maximizing the capacity. The capacity of an interference free channel is considered, often referred to as a noise limited scenario. The analysis is based on a large number of MIMO channel propagation measurements involving ten different practical handset designs in realistic use with different users and use cases (UCs). The measurements were carried out in a real micro-cellular propagation environment in an indoor environment, with two dual-band BSs operating simultaneously.

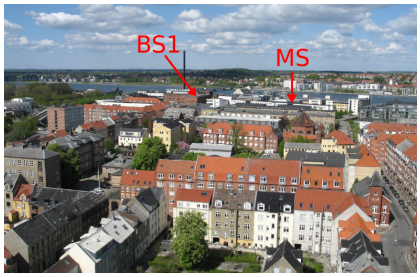

(a) (b)

Fig. 1: (a) View from BS2 towards the measurement location. (b) BS1 mounted on lift.

The measurements are described in Section II and the data processing and figures of merits are defined in Section III. The results are discussed in Section IV, followed by conclusions in Section V.

II. Measurements

The measurements were made in a micro-cellular setup with two BSs in the city of Aalborg, Denmark, and with the MSs on the top floor of a three-story office building. Both BSs are equipped with two antennas on two bands and all handsets have two antennas, so that MIMO operation can be evaluated. Ten different handsets were measured in FS, with phantoms, and with users.

The measurements were carried out using a wide band MIMO channel sounder [30], allowing truly simultaneous measurements of the channels from all four low band (LB) and four high band (HB) transmitter (Tx) antennas on the two base stations, to four dual-band receiver (Rx) antennas in the handsets. Four handsets were measured at the same time, each with two antennas connected via a 2:1 multiplexing switch. The switch operates fast enough to be considered negligible in the total measurement time for one full MIMO channel sample of about 164 μs. Assuming a max speed of 1 m/s, this measurement duration corresponds to a max phase error of about 0.5°.

Since all Rx channels are dual-band, the overall size of the measured MIMO channel was 8×16 (Tx $\times$ Rx). The wide band channel matrix was measured at a rate of 60 Hz to cope with channel changes due to the movements of the users and other changes in the channel.

The measurement campaign for the current work was similar to the one described in [17], but with some important differences. The campaign is outlined in Table I, where reference is made to the handsets labelled H1, H2,..., H6, H11, ..., H14, which are described further in Section II-A below. Fig. 1 and Fig. 2 illustrate the measurements.

A. Handsets

The ten handsets used in this work are mock-ups specially designed to be realistic with respect to antenna shape and size, electromagnetic properties, casing and handling. At the same time, the mock-ups allow for connection to the channel sounding equipment. Some of the handsets have been designed

Published in *IEEE Transactions on Antennas and Propagation*, Vol. 62, No. 6, p. 3232–3241, June 2014. DOI: 10.1109/TAP.2014.2309967.

TABLE I: Key characteristics of the measurement campaign.

Base stations	BS1 is located about 21 m above the ground on a lift (see Fig. 1b), with obstructed line of sight (LOS) to the measurement building about 150 m away. BS2 is located on top of a tall building at a height of about 60 m and overlooking the surrounding buildings, see Fig. 1a. BS2 has obstructed LOS to the measurement building about 500 m away.
Frequencies	Two bands were measured simultaneously; The low band (LB) at 796 MHz and high band (HB) at 2300 MHz using effective bandwidths of about 5 MHz and 30 MHz, respectively.
Tx antennas	Both BS1 and BS2 have two antennas at both the LB and the HB. All antennas are vertically polarized. The two antennas on the LB and the HB are separated by 1.92 m and 0.64 m, respectively, both corresponding to about 5 wavelengths.
Rx antennas	Each handset is equipped with two antennas, see Table II. The handsets are measured simultaneously in groups of four: G1 = {H6, H1, H2, H5}, G2 = {H6, H3, H4, H11}, G3 = {H6, H12, H13, H14}
Channel sampling	The MIMO channels are sampled at 60 Hz. Each measurement is 20 s long, corresponding to 1200 samples. The impulse responses (IRs) are sampled at 400 MHz, corresponding to a 2.5 ns sample separation in delay.
Users	In order to include the variation in the influence by the user's hand and body, measurements with different persons were performed. For the G1 set of handsets eight persons were measured for all UCs, while four persons where measured with the G2 and G3 sets.
Use Cases (UCs)	Data mode measurements were carried out with all handsets in landscape mode for left (LRHL), right (LRHR), and two hands (LRTH), and in portrait mode with right hand (PHR) and two hands (PTH). In addition, corresponding FS measurements were made with the handsets mounted on expanded polystyrene (EPS) at an angle of 45°. Thus, as common in the propagation literature, the term FS is used to mean without user, but otherwise in the same multipath environment.
Measurement (MS) Location	Large hallway/common room on the 3rd floor of a building mainly made of concrete. All measurements were made inside or around four squares with about 1 m side length. The squares were arranged in a cross centered in the room with size about 7×12 m. The squares are labeled A, B, C, D, as illustrated in Fig. 2.
Mobile Orientation & Movement	During the measurements the user and handset moved randomly inside all of the square, but keept the same posture and orientation with respect to the environment. Each square A–D represents different orientations, separated by 90°.
Repetitions	Repetitions are used to estimate the measurement uncertainty due to various non-ideal conditions (see Section IV-A). The number of repetitions depends on the UC and handset, with most repetitions made in FS. In FS the landscape/right, right hand (LRHR) UC was repeated 4–5 times for most measurements, depending on the handset, but for data mode portrait (DMP) 13–40 repetitions were made for the handsets groups G1 and G2.

to mimic typical devices on the market while others are more experimental. All of the handsets are made in PC-ABS plastics using a 3D rapid prototyping printer, allowing for a very accurate mechanical design and natural user handling.

An overview of the handsets is given in Table II. Note that in addition to H6, another handset, H6r, is created by using

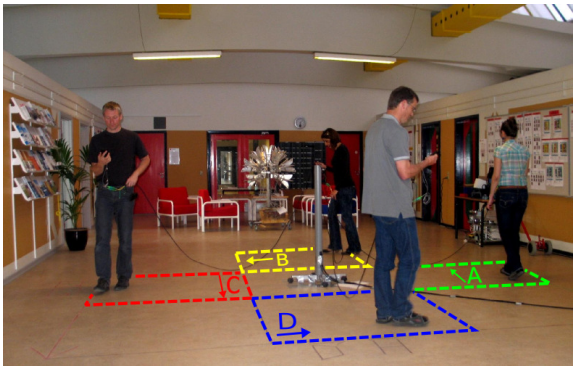

Fig. 2: Users during measurements, with the user squares and orientations A–D indicated, as described in Table I.

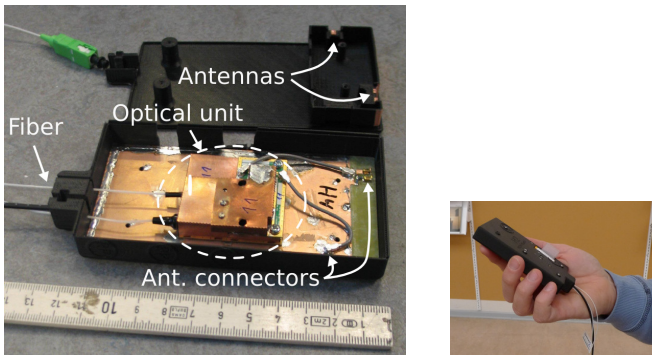

(a) (b)

Fig. 3: (a) Handset without cover. (b) Handset H2 used in right hand.

H6 upside-down. This is relevant for H6, since the influence of the users is expected to be significantly different due to the location of the antennas in that handset.

All of the handsets were connected to the sounding equipment via optical fibers, thereby avoiding the problems associated with using regular coaxial cables, such as changing the electromagnetic properties of the devices and making controlled measurements difficult. These problems are detailed further in [17] while [31] describes the optical units. Fig. 3 shows the internals of a handset and one in use.

III. Data Processing

Different MIMO constellations are possible based on the measurements described in the previous section. The following are considered in this work,

- BS1LB The two LB Tx branches from BS1 are used to form a 2×2 MIMO setup for each handset.
- BS1HB Similarly, the two HB Tx branches from BS1 are used to form a 2×2 MIMO setup.
- BS2LB The two LB Tx branches from BS2 are used to form a 2×2 MIMO setup for each handset.
- BS2HB Similarly, the two HB Tx branches from BS2 are used to form a 2×2 MIMO setup.

The MIMO channel is described by the matrix $H_i^r(m)$ consisting of the elements $h_i^r(p,q,m)$ where indices denote,

Published in *IEEE Transactions on Antennas and Propagation*, Vol. 62, No. 6, p. 3232–3241, June 2014. DOI: 10.1109/TAP.2014.2309967.

TABLE II: The handsets used in the measurement campaign, with form factor definitions according to [32]. Maximum electrical sizes of the antennas are given, *i.e.*, excluding the surrounding plastics of around 1.5 mm thickness.

Handset	Elec. size [mm]	Ant. No.	Ant. Type	Location	Low band	High band
H1	59×111	Rx1	ILA	Bottom	✓	✓
PDA		Rx2	ILA	Top	✓	✓
H2	59×111	Rx1	Mono	Top-Side/R	✓	✓
PDA		Rx2	Mono	Bottom-Side/R	✓	✓
H3	59×111	Rx1	Mono	Top-Side/R	✓	✓
PDA		Rx2	Mono	Bottom-Side/R	✗	✓
H4	59×111	Rx1	ILA	Top	✗	✓
PDA		Rx2	Mono	Top-Side/R	✓	✓
H5	59×111	Rx1	Mono	Top-Side/L	✓	✓
PDA		Rx2	Mono	Top-Side/R	✓	✓
H6	59×111	Rx1	ILA	Top	✓	✓
PDA		Rx2	Mono	Side/L	✓	✓
H6r	59×111	Rx1	ILA	Bottom	✓	✓
PDA		Rx2	Mono	Side/R	✓	✓
H11	59×111	Rx1	PIFA	Top	✓	✓
PDA		Rx2	PIFA	Bottom	✓	✓
H12	40×100	Rx1	PIFA	Top	✓	✓
Bar		Rx2	PIFA	Bottom	✓	✓
H13	59×111	Rx1	Helix	Top/L	✓	✗
PDA		Rx2	Helix	Bottom/L	✓	✗
H14	40×100	Rx1	Mono	Top/L	✓	✗
Bar		Rx2	Mono	Top/R	✓	✗

respectively, the p-th Rx antenna branch, the q-th Tx antenna branch, and the m-th time index. The i-index specifies a combination of the MIMO constellation, handset, orientation/location, repetition number, user, and UC (see the overview in Table I), where each combination results in a different MIMO channel measurement. For brevity, the combination details are omitted in the following description. The superscript r indicates a raw/un-normalized measurement. The scalar $h_i^r(p,q,m)$ is the complex gain of the narrow-band channel between the Tx and Rx branches, obtained via discrete Fourier transforms of the measured complex impulse responses (IRs).

To ensure a fair comparison, the channels are normalized to the mean power of all handsets in FS. The mean is computed independently for every Tx branch, mainly to remove path loss differences due to the distance and frequency. The FS average power gain for the q-th Tx branch is computed as

$$\Lambda(q) = \frac{1}{PMI}\sum_{p=1}^{P}\sum_{m=1}^{M}\sum_{i=1}^{I}|h_i^r(p,q,m)|^2 \tag{1}$$

where $P=2$ is the number of Rx branches of the handsets, and $M=1200$ is the number of narrow-band samples in each measurement. The averaging is done over I combinations of handset, orientation, UC, *etc.* The normalized channel matrix $H_i(m)$ has the elements

$$h_i(p,q,m) = \frac{h_i^r(p,q,m)}{\sqrt{\Lambda(q)}} \tag{2}$$

where $h_i^r(\cdot)$ is the un-normalized complex gain.

With the above normalized narrow-band channel, the signal received by a handset can be described as $\mathbf{y}=\mathbf{Hs}+\mathbf{n}$, where $\mathbf{s}$ is the vector of transmitted symbols with length Q, $\mathbf{n}$ is a same size noise vector, and $\mathbf{H}$ is the $P\times Q$ random channel matrix. Assuming that the transmitter has no knowledge of the channel and no interference is present, the capacity of the channel is given by [1]

$$c_i(m) = \sum_{e=1}^{E}\log_2\left(1+\frac{\lambda_i(e,m)\rho}{Q}\right) \tag{3}$$

where $\lambda_i(e,m)$ is the e-th eigenvalue of the matrix $H_i(m)H_i(m)^H$ and $E=\min(P,Q)$. The number of Tx antennas for the constellation is given by Q and ρ is the SNR. Note that ρ is defined relative to the normalization in (2), computed using the average power over all FS measurements. If a given measurement, say for a specific handset including the losses for a user, has a different average power Λ^l, the capacity obtained with (3) equals that obtained by using the normalization Λ and a scaled SNR. Assuming the power difference is due to a pure scaling, the following refers to $\rho\Lambda^l/\Lambda$ as the resulting effective SNR.

The instantaneous channel capacity $c_i(m)$ is random and in the following the mean capacity (MC) is used as a measure of the capacity performance, *i.e.*,

$$\mu_i = \frac{1}{M}\sum_{m=1}^{M}c_i(m) \tag{4}$$

In order to characterize the capacity variation during a measurement, the capacity spread (CS) is defined as

$$\sigma_i = \chi_i^{90\%} - \chi_i^{10\%} \tag{5}$$

where χ_i^{α} is the α-level outage capacity estimated from the measured random capacity.

Following an approach similar to that used in [33], a Taylor series is used to rewrite the capacity in (3),

$$c_i(m) = \sum_{e=1}^{E}\log_2\left(\frac{\rho\lambda_i(e,m)}{Q}\right) - \sum_{n=1}^{\infty}\frac{(-1)^n}{n\ln(2)}\left(\frac{Q}{\rho\lambda_i(e,m)}\right)^n \tag{6}$$

where the series converges on the condition that $r_i(e,m) = Q/[\rho\lambda_i(e,m)] < 1$. The contribution of the eigenvalues for which $r_i(e,m)\geq 1$ to (3) are $\log_2[1+1/r_i(e,m)]\leq 1$ and hence in many cases will be insignificant compared to the terms for which $r_i(e,m)<1$. Simply omitting the terms corresponding to small eigenvalues, a lower bound for the MC is obtained as

$$\begin{aligned}\mu_i &\geq \frac{1}{M}\sum_{m=1}^{M}\sum_{e=1}^{J}\log_2\left(\frac{\rho\lambda_i(e,m)}{Q}\right)\\ &= \frac{\log_2(10)}{10}\cdot J\rho_{\mathrm{dB}} &\text{(7a)}\\ &\quad + \frac{1}{M}\sum_{m=1}^{M}\sum_{e=1}^{J}\log_2\left[\lambda_i(e,m)\right] - J\log_2(Q) &\text{(7b)}\end{aligned}$$

Published in *IEEE Transactions on Antennas and Propagation*, Vol. 62, No. 6, p. 3232–3241, June 2014. DOI: 10.1109/TAP.2014.2309967.

where the last term of (6) converges to $-\log_2[1+r_i(e,m)]$ and thus can be omitted. The term ρ_{dB} is the SNR in dB and J is the *effective channel rank* defined as the maximum e such that $Q < \rho\lambda_i(e,m)$, assuming the eigenvalues are sorted in decreasing order. It can be noted that for large SNR $J = \min(P,Q)$, and the approximation is identical to the one given in [34], where the first term of (7b) is defined as the channel *richness*. In the current work the name *effective richness* is used for the term since it here depends on J.

The linear relation of the lower bound in (7) shows that the SNR and thus the average power gain of the channel plays an important role for the capacity. However, the question of the tightness of the lower bound remains, since the capacity also depends on the eigenvalues and not only the total power. Note that the total instantaneous power may be written in terms of the eigenvalues as

$$\mathrm{Tr}\left[H_i(m)H_i^H(m)\right] = \sum_{p=1}^{P}\sum_{q=1}^{Q}|h_i(p,q,m)|^2 = \sum_{e=1}^{E}\lambda_i(e,m) \quad (8)$$

Typically the mean power is used to characterize the combination of the channel and the antenna, such as in the MEG [24], [35]. In the current work the total mean power (TMP) for the i-th configuration is defined as the sum of the power received by the P antennas, averaged over time and the Q Tx branches.

$$\gamma_i = \frac{1}{QM}\sum_{q=1}^{Q}\sum_{m=1}^{M}\sum_{p=1}^{P}|h_i(p,q,m)|^2 \quad (9)$$

Another typical antenna characteristic is the branch power ratio (BPR) which here, for the p-th Rx antenna, is defined as

$$\alpha_i(p,p') = \frac{1}{Q}\sum_{q=1}^{Q}\frac{\sum_{m=1}^{M}|h_i(p,q,m)|^2}{\sum_{m=1}^{M}|h_i(p',q,m)|^2} \quad (10)$$

where $p=2$ and $p'=1$ is used in the following, since all handsets have two antennas.

Correlation is also considered as being important for the capacity. The branch correlation coefficient (BCC) for the i-th handset measurement is defined here as

$$\delta_i(p,p') = \frac{1}{Q}\sum_{q=1}^{Q}\frac{\sum_{m=1}^{M}\hat{h}_i(p,q,m)\hat{h}_i^*(p',q,m)}{\left(\sum_{m=1}^{M}|\hat{h}_i(p,q,m)|^2\right)^{1/2}\left(\sum_{m'=1}^{M}|\hat{h}_i(p',q,m')|^2\right)^{1/2}} \quad (11)$$

where $\hat{h}_i(\cdot)$ is $h_i(\cdot)$ with the mean value subtracted, and where $p=2$ and $p'=1$ is again used in the following. Note that the complex correlation between signals originating from the same Tx branch is considered here, as the main interest is the change in the correlation due to the properties of the different handsets while the BS end of the link is unchanged.

IV. Results

A. Repeatability

In principle a repeated measurement with the same setup should yield the same results in terms of, *e.g.*, MC, but in practice this may not be the case for several reasons, including the following:

- Noise and other uncertainties in the measurement system.
- Differences in the handling of the handset, such as exact angle with respect to vertical, the location of the user's fingers. Even if the user is instructed to use the same grip, small changes are inevitable.
- Similarly, minor changes in, *e.g.*, the measurement route, orientation, and walking speed must be expected. Even if the environment is stationary in statistical sense within the local area of movement, only a finite set of samples are acquired resulting in variation in the estimated values of, *e.g.*, MC.
- Changes in the surrounding environment, such as due to persons walking by the measurement location.

In order to evaluate the variation, a number of repeated measurements have been studied. In particular the data mode portrait (DMP) UC is emulated in FS by mounting the handsets on a block of expanded polystyrene (EPS) at an angle of 45°. The block of EPS with the handsets is on top of a wheeled table and during the measurements the table is moved randomly within one of the different squares, A–D. Measurements with the G1 set of handsets are considered (see Table I) and all combinations of the four squares and the four handsets are included, all of which are repeated. In total 378 combinations are used in the statistics.

For every combination of MIMO constellation, handset, and square, all the repeated measurements are collected and the MC, TMP, BPR, and BCC values are computed according to (4), (9), (10), and (11), respectively. For each measure, the repeated measurements result in random samples which are normalized with the sample mean of the particular combination. The normalized values are grouped together and percentiles are estimated. Table III shows the results for the different measures and MIMO constellations. In general a quite good match is achieved with the TMP within about 0.9 dB in 90% of the cases, while the BPR is within about 1.8 dB, the BCC within about 0.1 and the MC within about 0.4 bit/s/Hz, all in 90% of the cases.

B. Relation Between mean capacity (MC) and Channel Characteristics

In this section the focus is on how the capacity of realistic handsets/channels is linked to the observed TMP, BPR, and BCC, which are typically used to characterize the antennas and channel. To this end, the measurements discussed in Section II are used for statistical analysis, where in total about 2,800 different combinations of handsets, orientations, users, UCs are included, of which about 1,000 are measured in landscape mode with a user, about 700 are in portrait mode with a user, and about 1,100 are in FS. The statistics are based on independent computation of the MC, TMP, BPR, and BCC for all of the about 2,800 measurements.

Published in *IEEE Transactions on Antennas and Propagation*, Vol. 62, No. 6, p. 3232–3241, June 2014. DOI: 10.1109/TAP.2014.2309967.

TABLE III: Percentiles for deviations from mean value in total mean power (TMP), branch power ratio (BPR), branch correlation coefficient (BCC) and mean capacity (MC), respectively, computed from repeated measurements

	Percentile	BS1LB	BS2LB	BS1HB	BS2HB
TMP	50%	0.31	0.38	0.25	0.31
[dB]	90%	0.74	0.87	0.62	0.76
BPR	50%	0.60	0.70	0.39	0.48
[dB]	90%	1.77	1.73	1.08	1.22
BCC	50%	0.03	0.04	0.03	0.04
[-]	90%	0.10	0.12	0.08	0.10
MC	50%	0.16	0.16	0.12	0.10
[bit/s/Hz]	90%	0.35	0.35	0.31	0.25

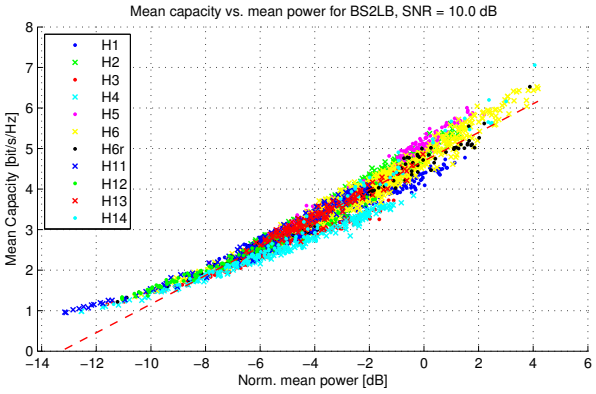

(a)

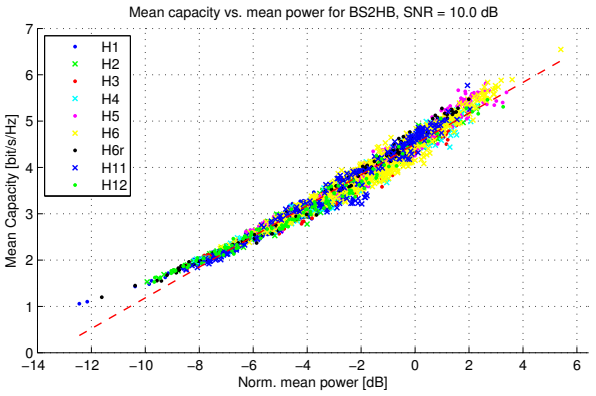

(b)

Fig. 4: Scatter plot of measured mean capacity (MC) versus total mean power (TMP) for (a) BS2LB and (b) BS2HB. The capacities are computed for an SNR of 10 dB.

Fig. 4 shows scatter plots of the MC versus the TMP, where each data point is computed using (9) and (4), assuming an SNR of 10 dB. Each point in the plot corresponds to one of the about 2,800 combinations of handset, orientation, user, UC, *etc.* The figure shows plots for the BS2LB and BS2HB constellations; similar results are obtained for BS1LB and BS1HB.

Note that, as described in Section III, the channels are normalized to the mean power in FS which means that the majority of measurements have a TMP less than 0 dB

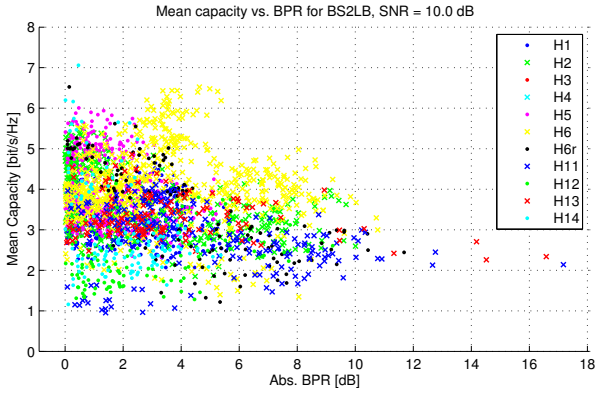

(a)

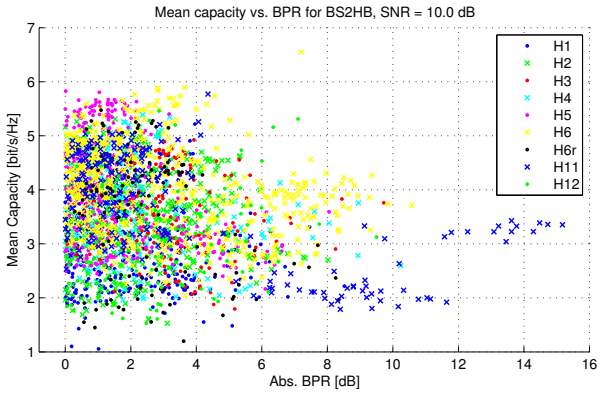

(b)

Fig. 5: Scatter plot of measured mean capacity (MC) versus absolute branch power ratio (BPR) for (a) BS2LB and (b) BS2HB. The capacities are computed for an SNR of 10 dB.

due to the body loss of the user, which is present in most measurements.

From the figures the MC appears strongly dependent on the TMP and thus the effective SNR in the channel, where the curved overall shape formed by the points may be explained by the logarithm in the capacity formula (3). Within the observed range of TMP the dependence is roughly linear, as shown by the dashed lines which are linear least squares fits to the scatter points.

The lower bound in (7) is linear with a slope given by $\log_2(10)/10J \simeq 0.33J$, where J is the effective rank of the channel. The slope of the least square fits in Fig. 4 are 0.35 and 0.33 for BS2LB and BS2HB, respectively, thus indicating that the effective rank equals one for the 10 dB SNR. However, it should be emphasized that the observed capacity values are *not* the result of varying the SNR parameter, ρ, of (3). Instead, the measurements with different channel/antenna combinations result in effective changes in the SNR, due to changes in the eigenvalues, see (8). The plots indicate that although the measurements have different eigenvalues, these changes show mainly as changes in the effective SNR for the capacities.

Similar scatter plots are shown in Fig. 5 where the MC is plotted versus the absolute BPR, again for BS2LB and BS2HB. Here it is noticed that for most (about 90%) of the

Published in *IEEE Transactions on Antennas and Propagation*, Vol. 62, No. 6, p. 3232–3241, June 2014. DOI: 10.1109/TAP.2014.2309967.

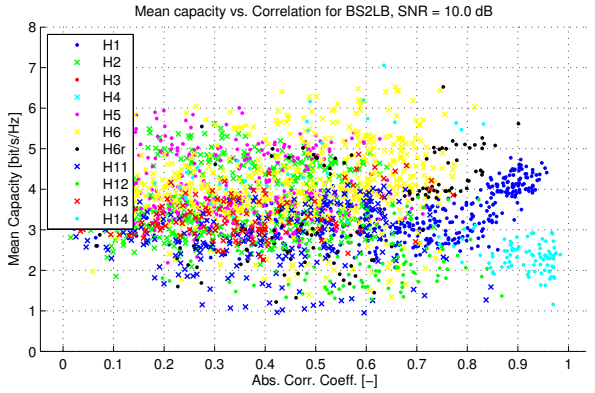

(a)

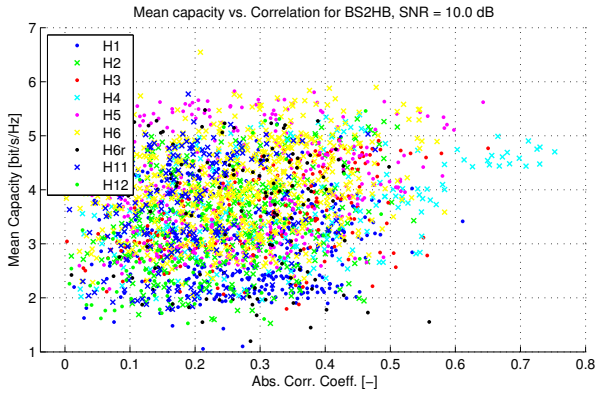

(b)

Fig. 6: Scatter plot of measured mean capacity (MC) versus absolute branch correlation coefficient (BCC) between Rx branches for (a) BS2LB and (b) BS2HB. The capacities are computed for an SNR of 10 dB.

measurements the BPR is less than 6 dB and that the MC appears weakly correlated to the BPR. This corresponds well with the investigations in [21], based on simulations, showing that a BPR of 6 dB corresponds to less than 3 dB change in SNR, and a BPR of 3 dB corresponds to less than 1.5 dB of change in SNR.

Fig. 6 shows the scatter plots for MC versus BCC for BS2LB and BS2HB. From the figure it is noticed that for the LB almost any value below 0.9 of the BCC has been measured, but the MC in general shows only a weak dependence. Note that a relatively high MC may be observed together with a high correlation if combined with a high TMP. This, however, is not a general tendency, since the TMP and BCC has a low correlation, see Table IV.

A high correlation between the antenna outputs may potentially decrease the capacity, as it was concluded from model based investigations in [18]. However, the work in [20] concludes, for dipoles in an isotropic environment, that complex correlation values below 0.5 hardly affects the capacity. Even for values up to 0.75 the capacity change is relatively small, less than the change caused by a 2 dB reduced SNR. This agrees well with the weak correlation between MC and the BCC, since most of the observed BCC values are less than 0.75.

TABLE IV: Correlation coefficient between different parameters. The capacities are computed for an SNR of 10 dB.

	BS1LB	BS2LB	BS1HB	BS2HB
MC & TMP	0.96	0.97	0.99	0.99
MC & BPR	−0.21	−0.24	−0.28	−0.21
MC & BCC	−0.08	−0.10	0.13	0.17
TMP & BPR	−0.12	−0.18	−0.19	−0.13
BPR & BCC	−0.10	−0.13	0.08	−0.03
TMP & BCC	0.06	0.00	0.17	0.20

For the HB the majority of the channels may be considered weakly correlated, with BCC most values below 0.5. Furthermore, no clear correlation exists between the MC and the BCC.

For comparison, it may be noted that Harryson *et al* [4] found the BCC to be less than 0.8 in about 90% of the cases for measurements made around 2.6 GHz with a personal digital assistant (PDA) type mockup handset with four planar inverted-F antenna (PIFA) elements, both in FS and mounted on a phantom. On the other hand, Michalopoulou *et al* [9] found the BCC close to 0.1 for simulated antennas at 1800 MHz, both in FS and with a cylinder shaped model of the user's body. Plicanic *et al* [10] obtained envelope BCC of up to 0.57 in FS and 0.45 with a phantom head and hand (next to head), both for integrated antennas of a PDA-type handset and assuming a uniform APD at 870 MHz. BPRs between 2 dB and 4 dB were observed.

Using propagation measurements with mockup-up devices, Yanakiev *et al* report (envelope) BCCs for two bands [25]. Low BCCs were found for 2.3 GHz, where three handsets had 95%-percentiles less than 0.32 both in FS and with users. For measurements in the 776 MHz band, BCCs of 0.38 and 0.87 in FS were measured for two handsets, which was reduced to 0.52 and 0.64, respectively, when users were present.

The correlation coefficients between the different measured parameters are summarized in Table IV where an SNR of 10 dB is used to compute the capacities. It is firstly noticed that the correlation coefficients (CCs) are roughly independent of the MIMO constellation. As expected from Fig. 4, the MC is strongly correlated to the TMP with CCs above 0.96 in all cases, while the MC is negatively correlated to the BPR with CCs between -0.21 and -0.28. The MC and the BCC shows only relatively small CCs, less than ± 0.17.

Since the capacity depends on the SNR, the CCs may also depend on the chosen SNR. Fig. 7 shows the obtained CCs between the MC and the TMP, BPR, and BCC parameters, respectively, for SNRs in the range 0–30 dB.

The general tendency of the CC between the MC and the TMP (Fig. 7a) is a slight increase from 0 dB with peak around 5–10 dB, followed by a decrease in CC with increasing SNR. Two mechanisms may explain this. Firstly, for low SNR the curve for MC versus TMP is slightly curved (convex), as in Fig. 4, due to the logarithm in the capacity formula. The curvature tends to lower the CC. Secondly, for large SNR the differences in MC among the scatter points are larger, see example in Fig. 8, leading to a decreasing CC between the MC and the TMP.

Published in *IEEE Transactions on Antennas and Propagation*, Vol. 62, No. 6, p. 3232–3241, June 2014. DOI: 10.1109/TAP.2014.2309967.

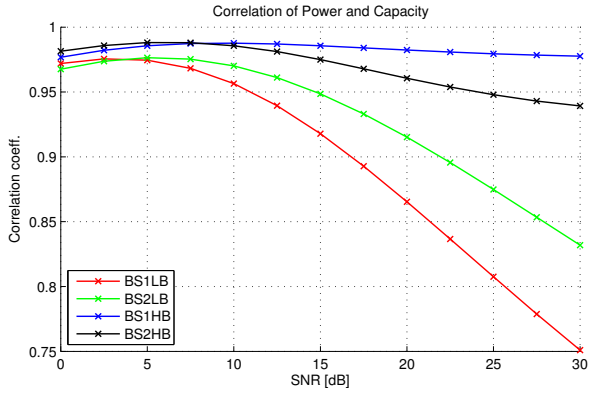

(a)

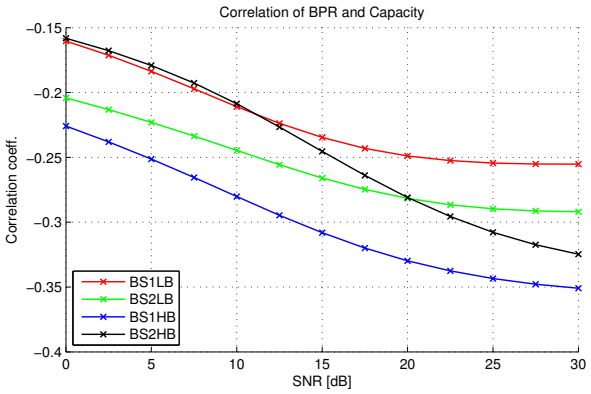

(b)

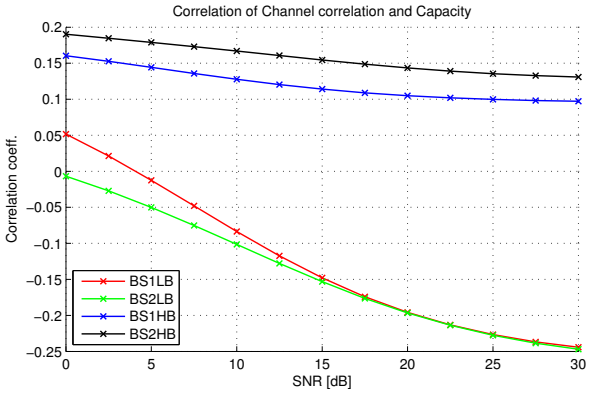

(c)

Fig. 7: Correlation coefficient versus SNR of mean capacity (MC) and (a) total mean power (TMP), (b) branch power ratio (BPR), and (c) branch correlation coefficient (BCC).

At the same time the absolute value of the CC between the BPR and the MC increases with SNR, as well as for the CC between the BCC and the MC, the latter only for the LB. Thus, when the SNR is growing the other parameters become more important, although seemingly at a decreasing rate and tending to a plateau.

The points in Fig. 8 corresponding to H4 are clearly visible in the lower part of the plot with a slope of roughly 0.3, giving an effective rank of about one. Similar is valid for H3. H3 and H4 both have a single antenna at the LB and therefore the

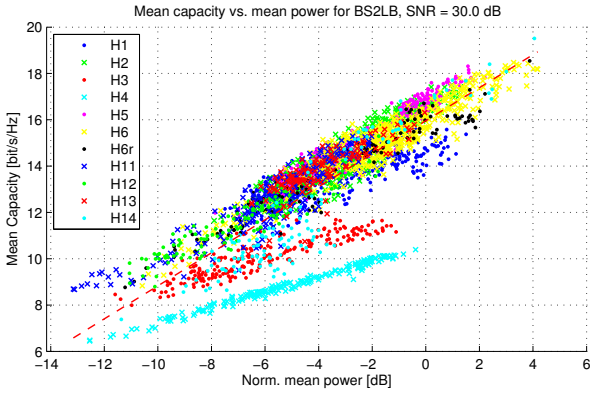

Fig. 8: Scatter plot of measured mean capacity (MC) versus total mean power (TMP) for BS2LB and an SNR of 30 dB.

maximum rank is one. In contrast, the slope of the regression line shown in Fig. 8 corresponds to an effective rank of about two. If H3/H4 are omitted from the analysis, the CCs between the TMP and MC are above 0.91 in all cases. The CCs for the BPR/MC and the BCC/MC are essentially unchanged.

C. Relation Between capacity spread (CS) and Channel Characteristics

The CS was defined in (5) as the difference between the 90%- and 10%-percentile of the instantaneous capacity. Examples of the obtained CS values are given in Fig. 9 in a scatter plot of the CS values versus the TMP for the channels from BS1LB to the handsets. It is found that the CS is within about 1–4 bits/s/Hz for an SNR of 10 dB, but the CS depends on the SNR. From Fig. 9 the CS is clearly correlated with the TMP. An overview of the correlation coefficients versus SNR is given in Fig. 10, where also curves for the correlation coefficients between CS and BCC, and between CS and BPR are given. All the curves are for BS1LB but the results are similar to those for BS2LB, BS1HB, and BS2HB.

The correlation between the CS and TMP generally decreases with increasing SNR, with values above 0.6 for 0–15 dB SNR. This is due to the variation in the CS which is generally increasing with increasing SNR.

A main observation is that the correlation coefficients between CS and BPR and between the CS and the BCC are generally low, with absolute values of 0.05–0.40.

V. Conclusion

The current work concerns the relation between the capacity and the total mean power (TMP), Rx branch power ratio (BPR), and the Rx branch correlation coefficient (BCC), respectively. The investigation is based on about 2,800 measurements of the MIMO channel between two vertically polarized BSs and 10 different handsets held by 4-8 test users in different use cases (UCs), also including free space (FS). The measurements were made with the users in one indoor environment.

The estimated correlation coefficient (CC) between the mean capacity (MC) and the TMP is generally high, with CC

Published in *IEEE Transactions on Antennas and Propagation*, Vol. 62, No. 6, p. 3232–3241, June 2014. DOI: 10.1109/TAP.2014.2309967.

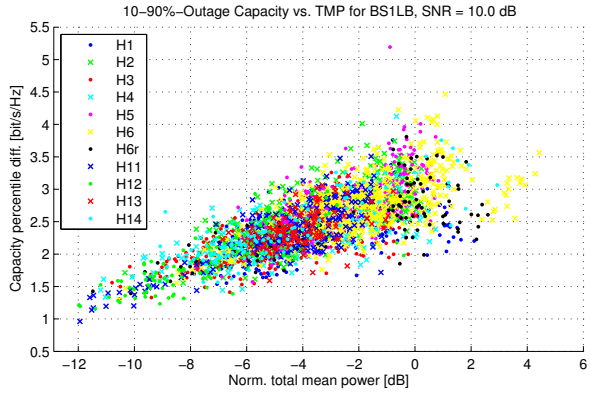

Fig. 9: Scatter plot of measured capacity spread (CS) versus total mean power (TMP) for BS1LB and an SNR of 10 dB.

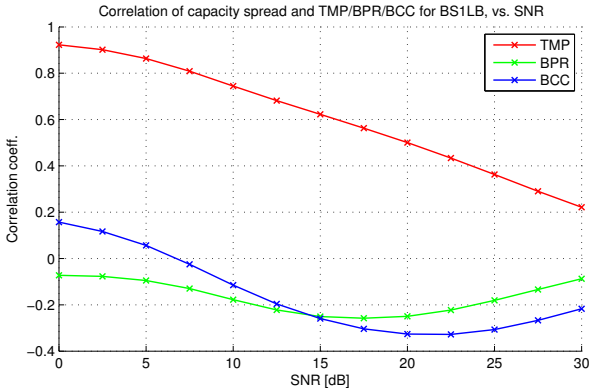

Fig. 10: Correlation of measured capacity spread (CS) and total mean power (TMP), branch power ratio (BPR), branch correlation coefficient (BCC), respectively, versus SNR and for BS1LB.

above 0.95 for an SNR of 10 dB and above 0.75 for 0–30 dB SNR. Conversely, the CC between both the MC and the BPR, and between the MC and BCC is relatively low. The absolute CC are in both cases less than 0.35 for an 0–30 dB SNR.

While both the BPR and the BCC are affecting the mean capacity in theory, the results show that for the practical handsets and live users involved in the selected setup, both the BCC and the BPR are in practice insignificant parameters in determining the MC of a realistic handset. As might be expected, the TMP is highly significant.

The capacity spread (CS), defined as the difference in the 90% and 10% outage capacity, is a measure of the capacity variation for each measurement. The CC of the CS and both the BCC and the BPR is generally low, less than about 0.35 (absolute values) for 0–30 dB SNR. The CC of TMP and CS, on the other hand, is about 0.9 for a 0 dB SNR, decreasing to about 0.2 for a 30 dB SNR. The decrease in the CC is due to larger variation in the CS among the measurements for an increased SNR.

Acknowledgements

The authors would like to thank Professor C. Luxey and A. Diallo at the University of Nice Sophia-Antipolis, France and I. Dioum at Université Cheikh Anta Diop de Dakar, Sénégal for developing the special decoupling technique [36] and designing the antenna used in one of the handsets.

References

[1] D. Gesbert, M. Shafi, D. shan Shiu, P. J. Smith, and A. Naguib, "From theory to practice: An overview of MIMO space-time coded wireless systems," *IEEE J. Sel. Areas Commun.*, vol. 21, no. 3, pp. 281–302, Apr. 2003.

[2] T. Paul and T. Ogunfunmi, "Evolution, insights and challenges of the PHY layer for the emerging IEEE 802.11n amendment," *IEEE Commun. Surveys Tutor.*, vol. 11, no. 4, pp. 131–150, quarter 2009.

[3] D. Astély, E. Dahlman, A. Furuskär, Y. Jading, M. Lindström, and S. Parkvall, "LTE: the evolution of mobile broadband," *IEEE Commun. Mag.*, vol. 47, no. 4, pp. 44–51, Apr. 2009.

[4] F. Harrysson, J. Medbo, A. Molisch, A. Johansson, and F. Tufvesson, "Efficient experimental evaluation of a MIMO handset with user influence," *IEEE Trans. Wireless Commun.*, vol. 9, no. 2, pp. 853–863, Feb. 2010.

[5] M. Murase, Y. Tanaka, and H. Arai, "Propagation and antenna measurements using antenna switching and random field measurements," *IEEE Trans. Veh. Technol.*, vol. 43, no. 3, pp. 537–541, Aug. 1994.

[6] G. F. Pedersen, J. Ø. Nielsen, K. Olesen, and I. Z. Kovacs, "Measured variation in performance of handheld antennas for a large number of test persons," in *48th Vehicular Technology Conf., VTC '98.* IEEE, May 1998, pp. 505–509.

[7] F. Harrysson, A. Derneryd, and F. Tufvesson, "Evaluation of user hand and body impact on multiple antenna handset performance," in *Antennas and Propagation Society Int. Symp. (APSURSI), 2010 IEEE*, Jul. 2010, pp. 1 –4.

[8] T. Zervos, K. Peppas, F. Lazarakis, A. Alexandridis, K. Dangakis, and C. Soras, "Channel capacity evaluation for a multiple-input-multiple-output terminal in the presence of user's hand," *IET Microw., Antennas Propag.*, vol. 1, no. 6, pp. 1137 –1144, Dec. 2007.

[9] A. Michalopoulou, T. Zervos, A. Alexandridis, K. Peppas, F. Lazarakis, K. Dangakis, and D. Kaklamani, "The impact of the user's body on the performance of a MIMO terminal in "pocket position"," in *The Second European Conf. on Antennas and Propagation (EuCAP) 2007.*, Nov. 2007, pp. 1–7.

[10] V. Plicanic, B. K. Lau, A. Derneryd, and Z. Ying, "Actual diversity performance of a multiband diversity antenna with hand and head effects," *IEEE Trans. Antennas Propag.*, vol. 57, no. 5, pp. 1547–1556, May 2009.

[11] V. Plicanic, B. K. Lau, and Z. Ying, "Performance of a multiband diversity antenna with hand effects," in *Int. Workshop on Antenna Technology: Small Antennas and Novel Metamaterials (iWAT)*, 2008, pp. 534–537.

[12] Y. Okano and K. Cho, "Dependency of MIMO channel capacity on XPR around mobile terminals for multi-band multi-antenna," in *The Second European Conf. on Antennas and Propagation (EuCAP)*, 2007.

[13] C. Martin, J. Winters, and N. Sollenberger, "MIMO radio channel measurements: performance comparison of antenna configurations," in *Vehicular Technology Conf., 2001. VTC 2001 Fall. IEEE VTS 54th*, vol. 2, 2001, pp. 1225–1229 vol.2.

[14] P. Suvikunnas, J. Salo, L. Vuokko, J. Kivinen, K. Sulonen, and P. Vainikainen, "Comparison of MIMO antenna configurations: Methods and experimental results," *IEEE Trans. Veh. Technol.*, vol. 2, no. 57, pp. 1021–1031, Mar. 2008.

[15] K. Sulonen, P. Suvikunnas, L. Vuokko, J. Kivinen, and P. Vainikainen, "Comparison of MIMO antenna configurations in picocell and microcell environments," *IEEE J. Sel. Areas Commun.*, vol. 21, no. 5, Jun. 2003.

[16] V. Plicanic, H. Asplund, and B. K. Lau, "Performance of handheld MIMO terminals in noise- and interference-limited urban macrocellular scenarios," *IEEE Trans. Antennas Propag.*, vol. 60, no. 8, pp. 3901–3912, 2012.

[17] J. Ø. Nielsen, B. Yanakiev, I. Bonev, M. Christensen, and G. Pedersen, "User influence on MIMO channel capacity for handsets in data mode operation," *IEEE Trans. Antennas Propag.*, vol. 60, no. 2, pp. 633 –643, Feb. 2012.

[18] D. shan Shiu, G. Foschini, M. Gans, and J. Kahn, "Fading correlation and its effect on the capacity of multielement antenna systems," *IEEE Trans. Commun.*, vol. 48, no. 3, pp. 502–513, Mar. 2000.

[19] D. Gesbert, H. Bolcskei, D. Gore, and A. Paulraj, "Outdoor MIMO wireless channels: models and performance prediction," *IEEE Trans. Commun.*, vol. 50, no. 12, pp. 1926–1934, Dec. 2002.

Published in *IEEE Transactions on Antennas and Propagation*, Vol. 62, No. 6, p. 3232–3241, June 2014. DOI: 10.1109/TAP.2014.2309967.

[20] A. Derneryd, J. Friden, P. Persson, and A. Stjernman, "Performance of closely spaced multiple antennas for terminal applications," in *3rd European Conf. on Antennas and Propagation (EuCAP)*, 2009, pp. 1612–1616.
[21] R. Tian, B. K. Lau, and Z. Ying, "Multiplexing efficiency of MIMO antennas," *IEEE Antennas Wireless Propag. Lett.*, vol. 10, pp. 183–186, 2011.
[22] J. Salo, P. Suvikunnas, H. El-Sallabi, and P. Vainikainen, "Ellipticity statistic as measure of MIMO multipath richness," *Electron. Lett.*, vol. 42, no. 3, pp. 160–162, 2006.
[23] R. G. Vaughan and J. B. Andersen, "Antenna diversity in mobile communications," *IEEE Trans. Veh. Technol.*, vol. 36, no. 4, pp. 149–172, nov 1987.
[24] T. Taga, "Analysis for mean effective gain of mobile antennas in land mobile radio environments," *IEEE Trans. Veh. Technol.*, vol. 39, no. 2, pp. 117–131, May 1990.
[25] B. Yanakiev, J. Ødum Nielsen, M. Christensen, and G. Pedersen, "On small terminal antenna correlation and impact on MIMO channel capacity," *IEEE Trans. Antennas Propag.*, vol. 60, no. 2, pp. 689–699, Feb. 2012.
[26] F. Athley, A. Derneryd, J. Friden, L. Manholm, and A. Stjernman, "MIMO performance of realistic UE antennas in LTE scenarios at 750 MHz," *IEEE Antennas Wireless Propag. Lett.*, vol. 10, pp. 1337–1340, 2011.
[27] F. Athley, L. Manholm, J. Friden, and A. Stjernman, "Practical multi-antenna terminals in LTE system performance simulations," in *General Assembly and Scientific Symp., 2011 XXXth URSI*, 2011, pp. 1–4.
[28] B. Hagerman, K. Werner, and J. Yang, "MIMO performance at 700MHz: Field trials of LTE with handheld UE," in *IEEE Vehicular Technology Conf. (VTC Fall)*, 2011, pp. 1–5.
[29] K. Werner, J. Furuskog, M. Riback, and B. Hagerman, "Antenna configurations for 4x4 MIMO in LTE - field measurements," in *Vehicular Technology Conf. (VTC 2010-Spring), 2010 IEEE 71st*, 2010, pp. 1–5.
[30] J. Ø. Nielsen, J. B. Andersen, P. C. F. Eggers, G. F. Pedersen, K. Olesen, E. H. Sørensen, and H. Suda, "Measurements of indoor 16×32 wideband MIMO channels at 5.8 GHz," in *Proceedings of the 2004 Int. Symp. on Spread Spectrum Techniques and Applications (ISSSTA 2004)*, 2004, pp. 864–868.
[31] B. Yanakiev, J. Nielsen, M. Christensen, and G. Pedersen, "Long-range channel measurements on small terminal antennas using optics," *IEEE Trans. Instrum. Meas.*, vol. 61, no. 10, pp. 2749 –2758, Oct. 2012.
[32] Cellular Telecommunications & Internet Association (CTIA), "Test plan for mobile station over the air performance; method of measurement for radiated RF power and receiver performance. revision number 3.1," CTIA, Tech. Rep., Jan. 2011, available at http://www.ctia.org.
[33] J. Ø. Nielsen, J. B. Andersen, G. Bauch, and M. Herdin, "Relationship between capacity and pathloss for indoor MIMO channels," in *The 17th Annual IEEE Int. Symp. on Personal, Indoor and Mobile Radio Communications (PIMRC'06)*, 2006.
[34] J. B. Andersen and J. Ø. Nielsen, "Modelling the full MIMO matrix using the richness function," in *Proc. of the ITG/IEEE Workshop on Smart Antennas (WSA)*, Apr. 2005.
[35] J. Ø. Nielsen, B. Yanakiev, I. B. Bonev, M. Christensen, and G. F. Pedersen, "User influence on the mean effective gain for data mode operation of mobile handsets," in *6th European Conf. on Antennas and Propagation (EuCAP)*, Mar. 2012, pp. 2759–2763.
[36] A. Diallo, C. Luxey, P. Le-Thuc, R. Staraj, and G. Kossiavas, "Study and reduction of the mutual coupling between two mobile phone PIFAs operating in the DCS1800 and UMTS bands," *IEEE Trans. Antennas Propag.*, vol. 54, no. 11, pp. 3063–3074, Nov 2006.

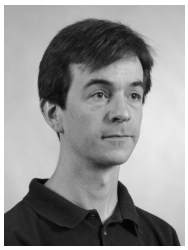

Jesper Ødum Nielsen received his master's degree in electronics engineering in 1994 and a PhD degree in 1997, both from Aalborg University, Denmark. He is currently employed at Department of Electronic Systems at Aalborg University where main areas of interests are experimental investigation of the mobile radio channel and the influence mobile device users have on the channel. He has been involved in MIMO channel sounding and modeling, as well as measurements using live GSM and LTE networks. In addition he has been working with radio performance evaluation, including over the air testing of active wireless devices.

Boyan Yanakiev received a bachelors degree in physics from Sofia University, Bulgaria in 2006 and a master's degree in Wireless Communication and a PhD degree from Aalborg University, Denmark in 2008 and 2011 respectively. His current position is as an antenna design engineer at Intel Mobile Communications and an industrial postdoctoral fellow at Aalborg University. His primary interests are in the area of design and evaluation of small integrated mobile antennas, optical antenna measurement techniques and radio channel measurements. He has been involved in the design and development of multiple RF-to-optical converters, for on-board handset measurements.

Samantha Caporal Del Barrio was born in 1987. After completing the scientific "Classes Prparatoires aux Grandes Ecoles" (CPGE), she entered a "Grande Ecole" in Paris, in 2005. There she received the B.Sc. degree in physics and pursued her M.Sc. degree in telecommunication engineering and mobile communications. She specialized in antennas and propagation at Aalborg University, Aalborg, Denmark. In 2010 she received the both M.Sc. degrees from Paris ECE Grande Ecole and Aalborg University. She is currently pursuing her Ph.D. degree in wireless communications at Aalborg University. Her research interests include small terminal performances, users influence on MIMO handsets and frequency-reconfigurable antennas for 4G implementation. She is also involved in the COST Action IC 1004 on "Cooperative Radio Communications for Green Smart Environments" and the COST Action IC 1102 on "Versatile, Integrated and Signal-aware Technologies for Antennas".

Published in *IEEE Transactions on Antennas and Propagation*, Vol. 62, No. 6, p. 3232–3241, June 2014. DOI: 10.1109/TAP.2014.2309967.

Gert Frølund Pedersen was born in 1965 and married to Henriette and have 7 children. He received the B.Sc. E. E. degree, with honour, in electrical engineering from College of Technology in Dublin, Ireland in 1991, and the M.Sc. E. E. degree and Ph. D. from Aalborg University in 1993 and 2003. He has been with Aalborg University since 1993 where he is a full Professor heading the Antenna, Propagation and Networking LAB with 36 researcher. Further he is also the head of the doctoral school on wireless communication with some 100 phd students enrolled. His research has focused on radio communication for mobile terminals especially small Antennas, Diversity systems, Propagation and Biological effects and he has published more than 175 peer reviewed papers and holds 28 patents. He has also worked as consultant for developments of more than 100 antennas for mobile terminals including the first internal antenna for mobile phones in 1994 with lowest SAR, first internal triple-band antenna in 1998 with low SAR and high TRP and TIS, and lately various multi antenna systems rated as the most efficient on the market. He has worked most of the time with joint university and industry projects and have received more than 12 M$ in direct research funding. Latest he is the project leader of the SAFE project with a total budget of 8 M$ investigating tunable front end including tunable antennas for the future multiband mobile phones. He has been one of the pioneers in establishing Over-The-Air (OTA) measurement systems. The measurement technique is now well established for mobile terminals with single antennas and he was chairing the various COST groups (swg2.2 of COST 259, 273, 2100 and now ICT1004) with liaison to 3GPP for over-the-air test of MIMO terminals. Presently he is deeply involved in MIMO OTA measurement.

Published in *IEEE Transactions on Antennas and Propagation*, Vol. 62, No. 6, p. 3232–3241, June 2014. DOI: 10.1109/TAP.2014.2309967.